

---

Article

Not peer-reviewed version

---

# Performance of a Nanoribbon Biosensor Sensitized with Aptamers and Antibodies upon Detection of HCVcoreAg

---

[Yuri Ivanov](#) , [Kristina Malsagova](#) , [Kristina Goldaeva](#) \* , [Tatyana Pleshakova](#) , Andrey Kozlov , Rafael Galiullin , Ivan Shumov , [Vladimir Popov](#) , Irina Abramova , Ekaterina Nevedrova , [Angelina Vinogradova](#) , Vadim Ziborov , Oleg Petrov , [Alexander Dolgorobodov](#) , Alexander Archakov

Posted Date: 13 October 2023

doi: [10.20944/preprints202310.0841.v1](https://doi.org/10.20944/preprints202310.0841.v1)

Keywords: HCVcoreAg; antibody; aptamer; nanoribbon biosensor; diagnostics



Preprints.org is a free multidiscipline platform providing preprint service that is dedicated to making early versions of research outputs permanently available and citable. Preprints posted at Preprints.org appear in Web of Science, Crossref, Google Scholar, Scilit, Europe PMC.

Copyright: This is an open access article distributed under the Creative Commons Attribution License which permits unrestricted use, distribution, and reproduction in any medium, provided the original work is properly cited.

Disclaimer/Publisher's Note: The statements, opinions, and data contained in all publications are solely those of the individual author(s) and contributor(s) and not of MDPI and/or the editor(s). MDPI and/or the editor(s) disclaim responsibility for any injury to people or property resulting from any ideas, methods, instructions, or products referred to in the content.

Article

# Performance of a Nanoribbon Biosensor Sensitized with Aptamers and Antibodies upon Detection of HCVcoreAg

Yuri D. Ivanov <sup>1,2</sup>, Kristina A. Malsagova <sup>1</sup>, Kristina V. Goldaeva <sup>1,\*</sup>, Tatyana O. Pleshakova <sup>1</sup>, Andrey F. Kozlov <sup>1</sup>, Rafael A. Galiullin <sup>1</sup>, Ivan D. Shumov <sup>1</sup>, Vladimir P. Popov <sup>3</sup>, Irina K. Abramova <sup>1</sup>, Ekaterina D. Nevedrova <sup>1</sup>, Angelina V. Vinogradova <sup>1</sup>, Vadim S. Ziborov <sup>1,2</sup>, Oleg F. Petrov <sup>2</sup>, Alexander Yu. Dolgoborodov <sup>2</sup> and Alexander I. Archakov <sup>1</sup>

<sup>1</sup> Institute of Biomedical Chemistry (IBMC), Moscow 119121, Russia; yurii.ivanov.nata@gmail.com (Y.D.I.); kristina.malsagova86@gmail.com (K.A.M.); t.pleshakova1@gmail.com (T.O.P.); rafael.anvarovich@gmail.com (R.A.G.); shum230988@mail.ru (I.D.S.); afkozlow@mail.ru (A.F.K.); ira.abramova.01@inbox.ru (I.K.A.); ziborov.vs@yandex.ru (V.S.Z.); alexander.archakov@ibmc.msk.ru (A.I.A.)

<sup>2</sup> Joint Institute for High Temperatures of Russian Academy of Sciences, 125412 Moscow, Russia; ofpetrov@ihed.ras.ru (O.F.P.); aldol@ihed.ras.ru (A.Y.D.).

<sup>3</sup> Rzhanov Institute of Semiconductor Physics, Siberian Branch of Russian Academy of Sciences, 630090 Novosibirsk, Russia; popov@isp.nsc.ru (V.P.P.)

\* Correspondence: goldaeva\_1996@mail.ru (K.V.G.)

**Abstract:** The performance of the nanoribbon biosensor upon the use of two different types of molecular probes — the antibodies and the aptamers against HCVcoreAg — has been tested. The sensor chips employed are based on “silicon-on-insulator structures”. Two different HCVcoreAg preparations have been tested: recombinant  $\beta$ -galactosidase-conjugated HCVcoreAg (“Virogen”, USA) and recombinant HCVcoreAg (“Vector-Best”, Russia). Upon the detection of either type of the antigen preparation, the lowest concentration of the antigen detectable in buffer with pH 5.1 has been found to be approximately equal, amounting to  $\sim 10^{-14}$  M. This value has been found to be similar upon the use of either type of molecular probes.

**Keywords:** HCVcoreAg; antibody; aptamer; nanoribbon biosensor; diagnostics

---

## 1. Introduction

Hepatitis caused by the hepatitis C virus (HCV) represents an urgent problem of public health [1,2]. Globally, more than 170 million people are infected with HCV [3]. This virus has been known since 1989. Despite the tremendous advances achieved in treatment of this disease over the past decades, many patients may still remain difficult to treat [4,5]. The well-studied structure of HCV core proteins allows one to use them as biomarkers [6–8].

HCV core antigen (HCVcoreAg) is a marker protein used for the detection of HCV. This protein is found both in complete HCV virions and in RNA-less core protein structures [9]. The primary sequence of HCVcoreAg is highly conserved among all the different genotypes of the virus [31]. HCVcoreAg appears in blood 10–15 days after infection with HCV (1–2 days later than HCV RNA), thus not hindering early diagnosis of the disease [10,11]. This is why HCVcoreAg represents a promising protein marker for early revelation of HCV. Worldwide, a wide variety of different analytical systems for the detection of HCVcoreAg was proposed [12–14].

To date, enzyme linked immunosorbent assay (ELISA)-based methods of HCVcoreAg detection are routinely used in clinical practice [15]. Once again, it is the early diagnosis of HCV infection what the use of HCVcoreAg as a marker is promising. And the most serious drawback of ELISA-based assays is the lack of sensitivity [16,17]. With regard to early diagnosis of diseases, methods with at

least femtomolar (or, better, sub-femtomolar) detection limits are required [17]. In this regard, nanotechnology-based methods are the way to overcome this detection limit threshold [18]. Among these methods, nanowire and nanoribbon-based systems should be singled out [18]. These systems have numerous advantages. The first one is the label-free detection [19]. Furthermore, the presence of multiple sensor elements (i.e., an array of nanowires or nanoribbons) on a single sensor chip provides multiplexed detection [20]. The third advantage is that these biosensors allow one to detect the target analyte within ~15-20 minutes in a small sample volume [19]. Owing to these advantages, this type of biosensors has found its applications for highly sensitive real-time detection of a number of various types of analytes (such as nucleic acids, proteins, and viral particles) at low and ultra-low (femto- and subfemtomolar) concentrations, as was demonstrated in numerous papers [21–34]. This explains why this type of biosensors is so attractive for use in early revelation of various diseases in humans.

In our present research, we have employed the nanoribbon biosensor-based approach for the detection of HCVcoreAg in order to compare the biosensor performance upon the use of different molecular probes used for the capturing of the target protein. Namely, either anti-HCVcoreAg aptamers or anti-HCVcoreAg antibodies have been employed in our biosensor experiments as nanoribbon-immobilized molecular probes against the target HCVcoreAg protein. Furthermore, two model samples of purified HCVcoreAg preparation, which were manufactured by either "Virogen" (USA) or "Vector-Best" (Russia), have been studied. In the biosensor, sensor chips based on the so-called "silicon-on-insulator" structures have been employed. These chips have been fabricated by photolithography and gas-phase etching. We have demonstrated that these sensor chips, whose surface has been sensitized with either antibodies or anti-HCVcoreAg aptamers, can be successfully employed for label-free real-time detection of HCVcoreAg manufactured by "Virogen" or "Vector-Best" with virtually equal efficiency.

## 2. Materials and Methods

### 2.1. Reagents

The following reagents were used to pre-clean the sensing surface of the SOI-NW chip and perform its chemical modification: hydrofluoric acid (HF), 96% ethanol ( $C_2H_5OH$ ) ("Reakhim", Moscow, Russia), isopropanol, purified to 99.9% ( $C_3H_8O$ ) ("Acros Organics", Geel, Belgium), 3-aminopropyltriethoxysilane (APTES) ("Sigma Aldrich", St.-Louis, MO, USA) [30].

The sensitization of the nanoribbon surface with molecular probes was performed by their covalent immobilization onto the surface of individual nanoribbons using 3,3'-dithiobis(sulfosuccinimidyl propionate (DTSSP) ("Thermo Scientific", Waltham, MA, USA) as a crosslinker.

The following auxiliary compounds were also used in this study: potassium phosphate buffer (PPB) and potassium phthalate buffer (PPhthB).

Deionized water was purified using a Millipore Simplicity UV water purification system ("Millipore", Molsheim, France).

### 2.2. Anti-HCVcoreAg Antibodies

Murine monoclonal anti-HCVcoreAg antibodies (clone 1E5, specificity: the 1–80 a.a.r. region of the HCV core protein) ("Virogen", USA) were used.

The antibodies were specific to the regions of anti-HCVcoreAg antigens employed as target molecules.

### 2.3. Aptamers against HCVcoreAg

Anti-HCVcoreAg aptamers procured from "Evrogen" JSC (Moscow, Russia) with the sequence 5'-NH<sub>2</sub>-(T)<sub>10</sub>-  
ACGCTCGGATGCCACTACAGGCACGCCAGACCAGCCGTCCTCTTCATCCGAGCCTTCAC  
CGAGCCTCATGGACGTGCTGGTGA-3' [35] were employed.

#### 2.4. Antigens

The following antigens were employed in this study: (1) recombinant hepatitis C virus core protein (HCVcoreAg, 22 kDa) modified at the N-terminus with  $\beta$ -galactosidase (114 kDa) ("Virogen", USA), pI = 8.9; (2) recombinant hepatitis C virus core protein HCVcoreAg (kindly provided by O.N. Yastrebova, "Vector-Best", Russia).

#### 2.5. Preparing Buffer Solutions of HCVcoreAg

HCVcoreAg solutions within a concentration range from  $10^{-14}$  M to  $10^{-13}$  M were prepared from the initial protein solution (2  $\mu$ M in 50 mM PPB, pH 7.4) by tenfold serial dilution in 1 mM PPhthB (pH 5.1).

Each solution prepared was incubated in the shaker at 10°C for 30 min. Protein solutions were prepared immediately prior to the measurements.

#### 2.6. The Sensor Chips

The sensor chip is based on an ultrasensitive field-effect nanotransistor, in which the nanoribbon surface acts as a virtual gate [30,36]. Figure 1 displays a photographic image of the SOI-NW biosensor chip employed in our biosensor.

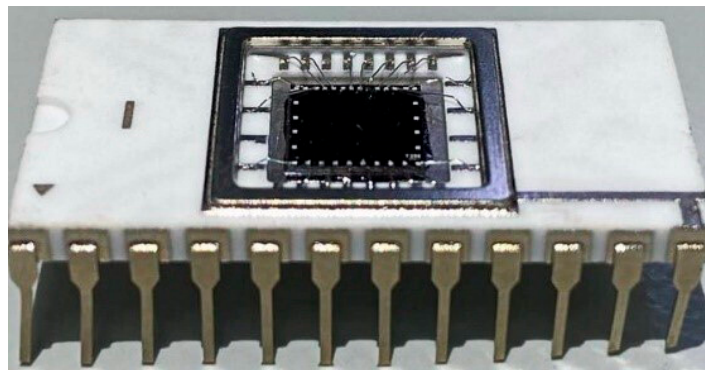


**Figure 1.** A photographic image of the SOI-NW chip.

The chips comprised five pairs of nanoribbons. The nanoribbons were 33  $\mu$ m wide, 32 nm thick, and 10  $\mu$ m long [37]. Thickness of the cut-off silicon layer and the buried oxide layer was 32 nm and 300 nm, respectively. The drain-source areas were formed by applying polysilicon layers followed by doping. The nanoribbon structures had n-type conductivity. Figure 2 displays a schematic drawing of the cross section of an individual nanoribbon.

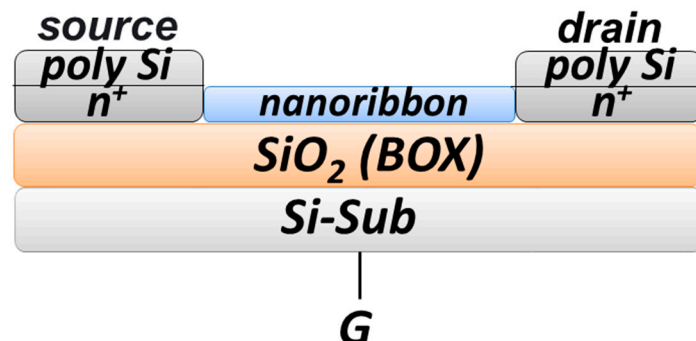


**Figure 2.** A schematic drawing of the cross-section of an individual nanoribbon based on the silicon-on-insulator structures.

### 2.7. Modification of the Surface of the SOI-SW Chip

Chemical modification of the sensing surface involved its pretreatment and further silanization with 3-aminopropyltriethoxysilane (APTES) analogously to the method developed by Yamada et al. [38] as described elsewhere [30,39].

At the pretreatment stage, mechanical impurities were removed from the chip surface by its rinsing with isopropanol ( $C_3H_7OH$ ). A solution containing hydrofluoric acid (HF) and ethanol ( $C_2H_5OH$ ) was further applied in order to remove any resting organic contaminants and, subsequently, the natural oxide [39,40], which was formed during storage of the chip [40].

In order to provide formation of hydroxyl groups the surface of the nanoribbons, the sensor chip was placed into a UV Ozone Cleaner (ProCleaner™ Plus, Ossila Ltd., Sheffield, UK) for 60 min. After these operations, vapour-phase silanization of the chip surface with APTES [38] was then carried out [30].

### 2.8. Sensitization of Individual Nanoribbons

The surface of individual nanoribbons was sensitized in order to provide biospecific detection; in other words, agents increasing the likelihood of selective binding between the analyzed molecules and the surface of the sensing element are applied onto the nanoribbon surface. These agents also ensure high sensitivity [41].

Sensitization was carried out by covalent immobilization of molecular probes of either type onto the surface of individual nanoribbons after the silanization of the sensor chip surface. DTSSP was used as a crosslinker for the immobilization [42]. The freshly prepared DTSSP solution was placed into a shaker and kept there at 10°C for 10 min; the solution was then dispensed onto the sensor chip surface and incubated thereon at 15°C and 80% humidity for 30 min. The chip surface was then rinsed ten times with 1 mL of deionized water. After that, solutions of either anti-HCVcoreAg antibodies or anti-HCVcoreAg aptamers were applied onto the surface of individual nanoribbons using a Piezoray dispensing system (PerkinElmer, Inc., Waltham, MA, USA). The dispensed volume was ~3 nL.

The nanoribbons with immobilized antibody or aptamer molecular probes were used as working nanoribbons, while nanoribbons without immobilized molecular probes were used as control ones.

### 2.9. The Biosensor Setup

A nanoribbon biosensor represents a system consisting of two modules: the analytical one and the electronic measuring one (Figure 3).

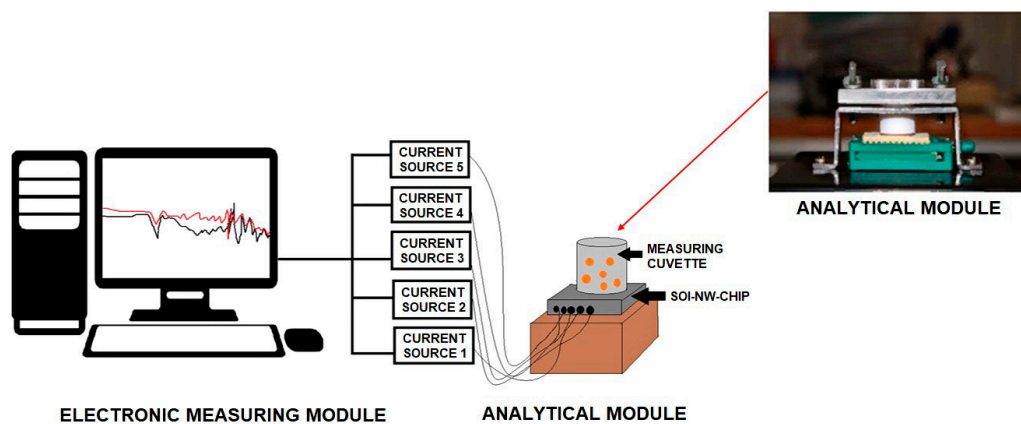


**Figure 3.** The schematic diagram of a NW-biosensor comprised of the analytical and electronic measuring modules.

The analytical module consisted of a liquid measuring cell (of 1000  $\mu\text{L}$  capacity), whose bottom was formed by the sensor chip.

The signal from the nanoribbons was received and recorded in real time by the electronic measuring module. This module allowed us to simultaneously record data from five nanoribbons on the one and the same sensor chip, and visualize the signal on a PC monitor during the experiment in real time. Analog-to-digital conversion of the recorded signal, as well as analysis and visualization of the measurement results, was performed using the TURBO NBS software (Rospatent registration No. 2015612969, February 27, 2015).

#### 2.10. Electrical Measurements

Electrical measurements were conducted using a Keithley picoammeter (Model 6487, Keithley Instruments Inc., USA). A substrate of the SOI structures was used as a gate during the measurements.

The nanoribbon biosensor system allows one to measure electrical signal in two modes:

1. The real-time mode: measuring  $I_{ds}(t)$  (recording drain–source current ( $I_{ds}$ ) vs. experiment duration ( $t$ ));
2. The mode of recording the current–voltage characteristics (CVC) of the nanoribbons: measuring  $I_{ds}(V_g)$  (recording drain–source current ( $I_{ds}$ ) vs. applied voltage ( $V_g$ )).

The working value of gate voltage (the working point)  $V_g$ , at which the drain–source current ( $I_{ds}$ ) was recorded, had been selected prior to performing the biosensor measurements. The working point was determined by measuring the current–voltage characteristics in a buffer solution. The  $I_{ds}(V_g)$  dependence was recorded within the voltage range from 0 to 60 V. Figure 4 displays typical CVC curves obtained in this way.

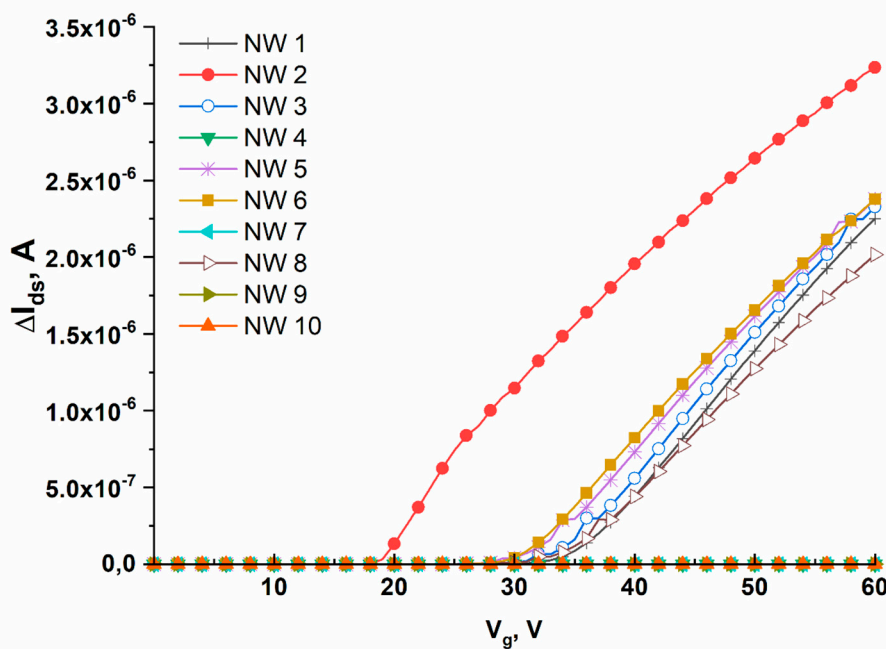


**Figure 4.** Typical CVC curves recorded for nanoribbons arranged on one and the same sensor chip. Experimental conditions:  $V_g = 0\text{--}60$  V,  $V_{ds} = 0.1$  V, PPhthB (pH 5.1).

In order to avoid the problems related to Debye shielding, the salt concentration in the buffer solutions, used in the biosensor experiments on the detection target protein, was low (1 mM). At this

concentration of buffer salts, the Debye length is  $\sim$ 12 nm, which is sufficient for detecting signal from HCVcoreAg on the nanoribbon surface [43,44].

Measurements were carried out at a constant voltage between the ohmic contacts of the nanoribbons (source–drain)  $V_{ds} = 0.1$  V and at operating gate voltage  $V_g = 45$  V. Once the measurement system was switched on, the cell was filled with the working solution and sequential measurements were then carried out: at the initial time interval before the test sample had been added; after the test solution had been added to the cell; and when the test solution in the cell was replaced with wash buffer.

### 2.11. Detection of HCVcoreAg with the Nanoribbon Biosensor

A sensor chip, whose individual nanoribbons were sensitized with either anti-HCVcoreAg antibodies or anti-HCVcoreAg aptamers as described above in section 2.8, was used in this study. In order to detect HCVcoreAg in purified buffer solution, 150  $\mu$ L of buffer solution of HCVcoreAg at concentration ranging from  $10^{-14}$  M to  $10^{-13}$  M was pipetted into the measuring cell containing 300  $\mu$ L of 1 mM buffer solution (PPhthB, pH 5.1). The measurements were conducted starting with the lowest concentration. After each test run, the sensor chip surface was washed with pure protein-free buffer (PPhthB, pH 5.1) and then, with warm deionized water (50 mL).

In the blank experiments, pure protein-free buffer (PPhthB, pH 5.1) was pipetted into the measuring cell instead of the HCVcoreAg solution. The sensor chip surface was washed with the same buffer, followed by washing with warm deionized water (50 mL).

### 2.12. Data Analysis

The data obtained in the real-time mode were presented as sensorgrams, which displayed time dependence of a dimensionless parameter expressed as arbitrary units.

Changes in the current  $I_{ds'}$  recorded for each nanoribbon, were first normalized to unity by dividing their values by the initial current. Next, in order to take into account the nonspecific interactions, the values obtained in the blank experiment were subtracted from the absolute data obtained with HCVcoreAg solution. The differential signal was then calculated by subtracting the signal for the control nanoribbon from the signal for the working nanoribbon. The resulting time dependencies of the current  $I_{ds}(t)$  were presented as sensorgrams showing the differential signal.

This data processing allowed us to account for the fact that the initial characteristics of currents flowing through different nanoribbons on one and the same sensor chip can differ. The initial currents for different nanoribbons may differ by one or two orders of magnitude. The standard deviation function was used to confirm the validity of the results.

## 3. Results

### 3.1. Detection of HCVcoreAg with the Use of Antibody Molecular Probes

We have performed the experiments on the HCVcoreAg detection with nanoribbons sensitized with anti-HCVcoreAg antibody probes. Two different HCVcoreAg preparations, produced by two different manufacturers, “Virogen” (USA) and “Vector-Best” (Russia) have been tested. Figure 5 displays typical sensograms obtained in the course of detection of HCVcoreAg at concentrations ranging from  $10^{-14}$  M to  $10^{-13}$  M in 1 mM PPhthB buffer (pH 5.1).

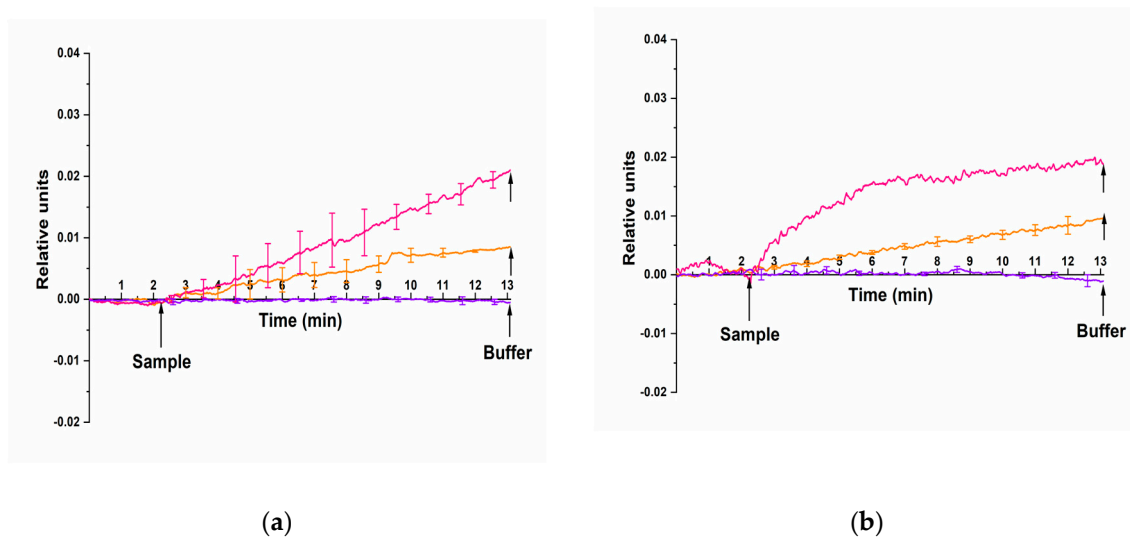


**Figure 5.** Typical sensograms illustrating the detection of HCVcoreAg with a nanoribbon biosensor sensitized with antibody probes. Two different HCVcoreAg preparations were tested: (a) HCVcoreAg manufactured by “Virogen”; (b) HCVcoreAg manufactured by “Vector-Best”. The HCVcoreAg concentration was  $10^{-14}$  M (orange curve) or  $10^{-13}$  M (pink curve). The data obtained in blank experiments for pure PPhthB containing no protein molecules are shown with a violet curve. The SOI-NW chip had n-type conductivity. Experimental conditions: 1 mM PPhthB;  $V_g = 45$  V,  $V_{ds} = 0.1$  V; solution volume in the measuring cell was 450  $\mu$ L. All measurements were performed in three technical replicates. Arrows indicate the time points of pipetting the HCVcoreAg solution into the cell and of sensor chip washing with pure buffer.

Figure 5 clearly shows that the addition of HCVcoreAg protein solutions manufactured by either “Virogen” (Figure 5a, orange and pink curves) or “Vector-Best” (Figure 5b, orange and pink curves) at concentrations ranging from  $10^{-14}$  M to  $10^{-13}$  M induced an increase in the conductivity of the nanoribbons sensitized with anti-HCVcoreAg antibody probes. This was caused by the positive charge of the target HCVcoreAg protein molecules under the experimental conditions at acidic pH 5.1. Accordingly, their binding to the probes immobilized on the surface of silicon nanoribbon altered its conductivity. We also observed an expected decrease in the level of the recorded signal upon decreasing the concentration of the target protein from  $10^{-13}$  M to  $10^{-14}$  M. Furthermore, the analysis of the blank solution revealed no change in conductivity of the antibody-sensitized nanoribbons (Figures 5a and 5b, violet curve), thus indicating it's the detection specificity.

The data obtained in our experiments indicated that recombinant HCVcoreAg manufactured by both “Virogen” and “Vector-Best” was detected using antibody molecular probes with comparable sensitivity. At that, the lowest concentration of HCVcoreAg detectable in buffer solution with pH 5.1 was determined to be  $10^{-14}$  M.

### 3.2. Detection of HCVcoreAg with the Use of Aptamer Molecular Probes

In the tests performed at this stage, similar to the experiments described above, two different HCVcoreAg preparations from “Virogen” (USA) and “Vector-Best” (Russia) were used. But the nanoribbons were sensitized with covalently immobilized aptamers instead of antibodies.

It was found that both antigen samples can be successfully detected in the solution using nanoribbons sensitized by aptamer probes. Figure 6 displays typical sensograms obtained in the course of detection of HCVcoreAg in the solution at concentrations ranging from  $10^{-14}$  M to  $10^{-13}$  M using n-type nanoribbons with immobilized aptamer probes.

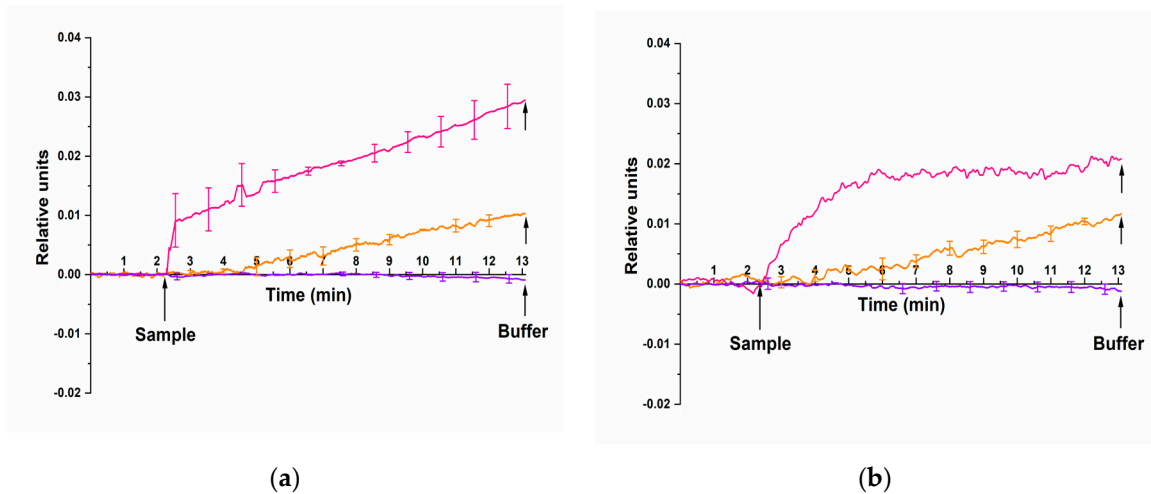


**Figure 6.** Typical sensograms illustrating the detection of HCVcoreAg with a nanoribbon biosensor sensitized with aptamer probes. Two different HCVcoreAg preparations were tested: (a) HCVcoreAg manufactured by “Virogen”; (b) HCVcoreAg manufactured by “Vector-Best”. The HCVcoreAg concentration was  $10^{-14}$  M (orange curve) or  $10^{-13}$  M (pink curve). The data obtained in blank experiments for pure PPhthB containing no protein molecules are shown with a violet curve. The SOI-NW chip had n-type conductivity. Experimental conditions: 1 mM PPhthB;  $V_g = 45$  V,  $V_{ds} = 0.1$  V; solution volume in the measuring cell was 450  $\mu$ L. All measurements were performed in three technical replicates. Arrows indicate the time points of pipetting the HCVcoreAg solution into the cell and of sensor chip washing with pure buffer.

The sensograms shown in Figure 6 indicate that upon addition of HCVcoreAg solutions at concentrations ranging from  $10^{-14}$  M to  $10^{-13}$  M the nanoribbon conductivity expectedly increases due to binding of positively charged HCVcoreAg antigen molecules with the aptamer-sensitized nanoribbon surface. This was observed for the both HCVcoreAg preparation tested, which were purchased from either “Virogen” (Figure 6a, orange and pink curves) or “Vector-Best” (Figure 6b, orange and pink curves). In contrast, the analysis of the blank solution revealed no change in the conductivity of aptamer-sensitized nanoribbons (Figures 6a and 6b, violet curve), being indicative of its specificity.

Thus, our analysis revealed comparable sensitivities of detecting recombinant HCVcoreAg procured from both “Virogen” and “Vector-Best” using immobilized aptamer probes ( $10^{-14}$  M).

#### 4. Discussion

Nanoribbon biosensor is a unique platform for high-sensitivity detection of protein molecules. It allows one to register signal, which corresponds to a level of a single molecule per the nanoribbon sensing element [45], since the latter has quite high surface-to-volume ratio [46].

Currently, ELISA and polymerase chain reaction (PCR) are the key methods used for diagnosing HCV [47–49]. One of the significant drawbacks of PCR is that data interpretation can be impeded (in particular, for the samples with viral loads below the quantitation limit) [50]. Moreover, PCR is quite sensitive to sample contamination — as opposed to the methods based on the detection of protein markers. Furthermore, relatively expensive equipment and reagents are required for PCR-based tests [51]. In turn, ELISA may yield false negative results in immunocompromised patients [52]. Furthermore, this analysis can yield low positive prognostic values in cohorts with low (<10%) prevalence of HCV infection [53,54]. In addition, as was noted in the Introduction ELISA allows one to detect biomarkers with concentration sensitivity of  $\sim 10^{-12}$  M [17], which is insufficient for diagnosing asymptomatic hepatitis C [17].

It is promising to use a nanoribbon biosensor as a universal platform for large-scale manufacturing of highly sensitive diagnostic systems available for personalized use owing to the ability of this biosensor to detect protein markers of infectious diseases with high sensitivity [55,56].

Our study reported has demonstrated that both anti-HCVcoreAg aptamer probes and anti-HCVcoreAg antibody probes, immobilized on the nanoribbon surface, have allowed us to successfully detect the target HCVcoreAg protein in buffer solutions at ultra-low concentrations ( $10^{-14}$  M). The conductivity of n-type nanoribbons expectedly increased when upon pipetting of HCVcoreAg solution into the measuring cell.

Hence, the detection sensitivity upon the use of aptamer molecular probes has been found to be comparable with that attained upon the use of antibodies. However, aptamer probes have a number of advantages over antibodies — namely, higher chemical, temperature, and time stability, and low production cost. Accordingly, aptamers are preferred to be used as molecular probes [57].

Furthermore, the detection sensitivities have been found to be comparable upon the use of either of the HCVcoreAg preparations produced by "Virogen" and "Vector-Best". It is also worth mentioning that the HCVcoreAg preparation produced by "Virogen" represented a conjugate of the target protein with  $\beta$ -galactosidase. This conjugate, accordingly, had higher molecular weight than the protein in the preparation manufactured by "Vector-Best". It is to be emphasized that under the conditions of our experiments, this fact did not affect the detection sensitivity. Furthermore, analysis of the blank solutions containing no HCVcoreAg revealed no changes in the nanoribbon conductivity, being indicative of its specificity.

## 5. Conclusions

In our biosensor experiments on the detection of HCVcoreAg protein with a nanoribbon biosensor, the nanoribbons were sensitized with covalently immobilized molecular probes of two types: antibodies and aptamers against HCVcoreAg. Furthermore, two different HCVcoreAg preparations have been tested. The first one was the  $\beta$ -galactosidase conjugate of recombinant HCVcoreAg produced by "Virogen" (USA). The second one was recombinant hepatitis C virus core protein HCVcoreAg (produced by "Vector-Best", Russia). The measurements have been carried out in the real-time mode and last ~15 min. Upon the use of either type of the antigen preparation in the experiments performed in purified buffer at pH 5.1, the lowest detectable concentration of the antigen was found to be approximately equal, amounting to  $\sim 10^{-14}$  M. This value was similar upon the use of either aptamer or antibody molecular probes. The biosensor used in our present study is a prototype of a unique test kit, which represents a molecular detector opening up new avenues for detecting target molecules in solutions at low and ultra-low concentrations. This biosensor allows one to perform early revelation of serological protein markers of socially significant diseases in humans, thus reducing the mortality rate as well as improve drug therapy efficacy and patients' quality of life.

**Author Contributions:** Conceptualization, Yuri Ivanov and Alexander Archakov; Data curation, Kristina Malsagova, Kristina Goldaeva and Irina Abramova, Ekaterina Nevedrova and Angelina Vinogradova; Formal analysis, Oleg Petrov; Funding acquisition, Alexander Archakov; Investigation, Kristina Malsagova, Kristina Goldaeva, Andrey Kozlov, Rafael Galiullin, Ivan Shumov, Irina Abramova and Vadim Ziborov; Methodology, Yuri Ivanov, Tatyana Pleshakova and Vladimir Popov; Project administration, Yuri Ivanov; Resources, Vladimir Popov, Vadim Ziborov, Oleg Petrov and Alexander Dolgorodov; Software, Rafael Galiullin; Supervision, Tatyana Pleshakova and Alexander Archakov; Validation, Vadim Ziborov; Visualization, Kristina Goldaeva, Andrey Kozlov and Ivan Shumov; Writing – original draft, Kristina Goldaeva and Ivan Shumov; Writing – review & editing, Yuri Ivanov. All authors have read and agreed to the published version of the manuscript.

**Funding:** The study was performed within the framework of the Program for Basic Research in the Russian Federation for a long-term period (2021-2030) (No. 122030100168-2).

**Data Availability Statement:** The data obtained throughout the experiments can be provided by Yu.D.I. upon reasonable request.

**Acknowledgments:** The biosensor measurements were performed employing a nanoribbon detector, which pertains to "Avogadro" large-scale research facilities.

**Conflicts of Interest:** The authors declare no conflict of interest.

## References

1. Ha, S.; Totten, S.; Pogany, L.; Wu, J.; Gale-Rowe, M. Hepatitis C in Canada and the Importance of Risk-Based Screening. *Can Commun Dis Rep* **2016**, *42* (3), 57–62. <https://doi.org/10.14745/ccdr.v42i03a02>.
2. Ullah, S.; Ali, S.; Daud, M.; Paudyal, V.; Hayat, K.; Hamid, S. M.; Ur-rehman, T. Illness Perception about Hepatitis C Virus Infection: A Cross-Sectional Study from Khyber Pakhtunkhwa Pakistan. *BMC Infect Dis* **2022**, *22* (1), 74. <https://doi.org/10.1186/s12879-022-07055-5>.
3. Lee, M.-H.; Yang, H.-I.; Lu, S.-N.; Jen, C.-L.; You, S.-L.; Wang, L.-Y.; Wang, C.-H.; Chen, W. J.; Chen, C.-J.; for the R.E.V.E.A.L.-HCV Study Group. Chronic Hepatitis C Virus Infection Increases Mortality From Hepatic and Extrahepatic Diseases: A Community-Based Long-Term Prospective Study. *Journal of Infectious Diseases* **2012**, *206* (4), 469–477. <https://doi.org/10.1093/infdis/jis385>.
4. Lauer, G. M.; Walker, B. D. Hepatitis C Virus Infection. *N Engl J Med* **2001**, *345* (1), 41–52. <https://doi.org/10.1056/NEJM200107053450107>.
5. Manns, M. P.; Maasoumy, B. Breakthroughs in Hepatitis C Research: From Discovery to Cure. *Nat Rev Gastroenterol Hepatol* **2022**, *19* (8), 533–550. <https://doi.org/10.1038/s41575-022-00608-8>.
6. Laperche, S.; Le Marrec, N.; Girault, A.; Bouchardieu, F.; Servant-Delmas, A.; Maniez-Montreuil, M.; Gallian, P.; Levayer, T.; Morel, P.; Simon, N. Simultaneous Detection of Hepatitis C Virus (HCV) Core Antigen and Anti-HCV Antibodies Improves the Early Detection of HCV Infection. *J Clin Microbiol* **2005**, *43* (8), 3877–3883. <https://doi.org/10.1128/JCM.43.8.3877-3883.2005>.
7. Pleshakova, T. O.; Kaysheva, A. L.; Shumov, I. D.; Ziborov, V. S.; Bayzyanova, J. M.; Konev, V. A.; Uchaikin, V. F.; Archakov, A. I.; Ivanov, Y. D. Detection of Hepatitis C Virus Core Protein in Serum Using Aptamer-Functionalized AFM Chips. *Micromachines* **2019**, *10* (2), 129. <https://doi.org/10.3390/mi10020129>.
8. Widell, A.; Molnegren, V.; Pieksma, F.; Calmann, M.; Peterson, J.; Lee, S. R. Detection of Hepatitis C Core Antigen in Serum or Plasma as a Marker of Hepatitis C Viraemia in the Serological Window-Phase. *Transfus Med* **2002**, *12* (2), 107–113. <https://doi.org/10.1046/j.1365-3148.2002.00359.x>.
9. Alonso, R.; Pérez-García, F.; López-Roa, P.; Alcalá, L.; Rodeño, P.; Bouza, E. HCV Core-Antigen Assay as an Alternative to HCV RNA Quantification: A Correlation Study for the Assessment of HCV Viremia. *Enfermedades infecciosas y microbiología clínica (English ed.)* **2018**, *36* (3), 175–178. <https://doi.org/10.1016/j.eimce.2016.11.008>.
10. Wang, Y.; Jie, W.; Ling, J.; Yuanshuai, H. HCV Core Antigen Plays an Important Role in the Fight against HCV as an Alternative to HCV-RNA Detection. *J Clin Lab Anal* **2021**, *35* (6). <https://doi.org/10.1002/jcla.23755>.
11. Kallala, O.; Kacem, S.; Fodha, I.; Pozzetto, B.; Abdelhalim, T. Role of Hepatitis C Virus Core Antigen Assay in Hepatitis C Care in Developing Country. *Egypt Liver J* **2021**, *11* (1), 77. <https://doi.org/10.1186/s43066-021-00146-z>.
12. Yousaf, M. Z.; Idrees, M.; Saleem, Z.; Rehman, I. U.; Ali, M. Expression of Core Antigen of HCV Genotype 3a and Its Evaluation as Screening Agent for HCV Infection in Pakistan. *Virol J* **2011**, *8* (1), 364. <https://doi.org/10.1186/1743-422X-8-364>.
13. Pérez-García, A.; Aguinaga, A.; Navascués, A.; Castilla, J.; Ezpeleta, C. Hepatitis C Core Antigen: Diagnosis and Monitoring of Patients Infected with Hepatitis C Virus. *International Journal of Infectious Diseases* **2019**, *89*, 131–136. <https://doi.org/10.1016/j.ijid.2019.09.022>.
14. Freiman, J. M.; Tran, T. M.; Schumacher, S. G.; White, L. F.; Ongarello, S.; Cohn, J.; Easterbrook, P. J.; Linas, B. P.; Denkinger, C. M. Hepatitis C Core Antigen Testing for Diagnosis of Hepatitis C Virus Infection: A Systematic Review and Meta-Analysis. *Ann Intern Med* **2016**, *165* (5), 345. <https://doi.org/10.7326/M16-0065>.
15. Ross, R.S. Analytical performance characteristics and clinical utility of a novel assay for total hepatitis C virus core antigen quantification. *J. Clin. Microbiol.* **2010**, *48*, 1161–1168. DOI: 10.1128/JCM.01640-09
16. Archakov, A.I.; Ivanov, Y.D.; Lisitsa, A.V.; Zgoda, V.G. Biospecific irreversible fishing coupled with atomic force microscopy for detection of extremely low-abundant proteins. *Proteomics* **2009**, *9*, 1326–1343. DOI: 10.1002/pmic.200800598.
17. Rissin, D. M.; Kan, C. W.; Campbell, T. G.; Howes, S. C.; Fournier, D. R.; Song, L.; Piech, T.; Patel, P. P.; Chang, L.; Rivnak, A. J.; Ferrell, E. P.; Randall, J. D.; Provuncher, G. K.; Walt, D. R.; Duffy, D. C. Single-Molecule Enzyme-Linked Immunosorbent Assay Detects Serum Proteins at Subfemtomolar Concentrations. *Nat Biotechnol* **2010**, *28* (6), 595–599. <https://doi.org/10.1038/nbt.1641>.
18. Barani, M.; Sabir, F.; Rahdar, A.; Arshad, R.; Kyzas, G.Z. Nanotreatment and Nanodiagnosis of Prostate Cancer: Recent Updates. *Nanomaterials* **2020**, *10*, 1696. <https://doi.org/10.3390/nano10091696>.
19. Stern, E.; Vacic, A.; Rajan, N.; Criscione, J.M.; Park, J.; Ilic, B.R.; Mooney, D.J.; Reed, M.A.; Fahmy, T.M. Label-free biomarker detection from whole blood. *Nat. Nanotech.* **2010**, *5*, 138–142. <https://doi.org/10.1038/nnano.2009.353>.
20. Zheng, G.; Patolsky, F.; Cui, Y.; Wang, W.U.; Lieber, C.M. Multiplexed electrical detection of cancer markers with nanowire sensor arrays. *Nat. Biotechnol.* **2005**, *23*, 1294–1301. <https://doi.org/10.1038/nbt1138>.

21. Patolsky, F.; Zheng, G.; Hayden, O.; Lakadamyali, M.; Zhuang, X.; Lieber, C. M. Electrical Detection of Single Viruses. *Proc. Natl. Acad. Sci. USA* **2004**, *101* (39), 14017–14022. <https://doi.org/10.1073/pnas.0406159101>.

22. Zhang, G.-J.; Zhang, G.; Chua, J. H.; Chee, R.-E.; Wong, E. H.; Agarwal, A.; Buddharaju, K. D.; Singh, N.; Gao, Z.; Balasubramanian, N. DNA Sensing by Silicon Nanowire: Charge Layer Distance Dependence. *Nano Lett.* **2008**, *8* (4), 1066–1070. <https://doi.org/10.1021/nl0729911>.

23. Zhang, G.-J.; Chua, J. H.; Chee, R.-E.; Agarwal, A.; Wong, S. M. Label-Free Direct Detection of MiRNAs with Silicon Nanowire Biosensors. *Biosensors and Bioelectronics* **2009**, *24* (8), 2504–2508. <https://doi.org/10.1016/j.bios.2008.12.035>.

24. Zhang, G.-J. Silicon Nanowire Biosensor for Ultrasensitive and Label-Free Direct Detection of MiRNAs. In *MicroRNA and Cancer*; Wu, W., Ed.; Methods in Molecular Biology; Humana Press: Totowa, NJ, 2011; Vol. 676, pp 111–121. [https://doi.org/10.1007/978-1-60761-863-8\\_9](https://doi.org/10.1007/978-1-60761-863-8_9).

25. Lu, N.; Gao, A.; Dai, P.; Li, T.; Wang, Y.; Gao, X.; Song, S.; Fan, C.; Wang, Y. Ultra-Sensitive Nucleic Acids Detection with Electrical Nanosensors Based on CMOS-Compatible Silicon Nanowire Field-Effect Transistors. *Methods* **2013**, *63* (3), 212–218. <https://doi.org/10.1016/j.ymeth.2013.07.012>.

26. Kim, A.; Ah, C. S.; Yu, H. Y.; Yang, J.-H.; Baek, I.-B.; Ahn, C.-G.; Park, C. W.; Jun, M. S.; Lee, S. Ultrasensitive, Label-Free, and Real-Time Immunodetection Using Silicon Field-Effect Transistors. *Appl. Phys. Lett.* **2007**, *91* (10), 103901. <https://doi.org/10.1063/1.2779965>.

27. Hung, J.-Y.; Manga, Y. B.; Chen, Y.-J.; Huang, H.-M.; Yang, W.-L.; Wu, C.-C. P16<sup>INK4a</sup> Detection Using an Ultra-Sensitive Silicon Nanowire Field Effect Transistor. In *2018 7th International Symposium on Next Generation Electronics (ISNE)*; IEEE: Taipei, 2018; pp 1–2. <https://doi.org/10.1109/ISNE.2018.8394715>.

28. Tian, R.; Regonda, S.; Gao, J.; Liu, Y.; Hu, W. Ultrasensitive protein detection using lithographically defined Si multinanowire field effect transistors. *Lab Chip* **2011**, *11* (11), 1952–1961.

29. Ivanov, Y.; Pleshakova, T.; Malsagova, K.; Kurbatov, L.; Popov, V.; Glukhov, A.; Smirnov, A.; Enikeev, D.; Potoldykov, N.; Alekseev, B.; Dolotkazin, D.; Kaprin, A.; Ziborov, V.; Petrov, O.; Archakov, A. Detection of Marker MiRNAs, Associated with Prostate Cancer, in Plasma Using SOI-NW Biosensor in Direct and Inversion Modes. *Sensors* **2019**, *19* (23), 5248. <https://doi.org/10.3390/s19235248>.

30. Ivanov, Y. D.; Pleshakova, T. O.; Kozlov, A. F.; Malsagova, K. A.; Krohin, N. V.; Shumyantseva, V. V.; Shumov, I. D.; Popov, V. P.; Naumova, O. V.; Fomin, B. I.; Nasimov, D. A.; Aseev, A. L.; Archakov, A. I. SOI Nanowire for the High-Sensitive Detection of HBsAg and  $\alpha$ -Fetoprotein. *Lab Chip* **2012**, *12* (23), 5104–5111. <https://doi.org/10.1039/c2lc40555e>.

31. Ivanov, Y. D.; Malsagova, K. A.; Popov, V. P.; Pleshakova, T. O.; Kozlov, A. F.; Galiullin, R. A.; Shumov, I. D.; Kapustina, S. I.; Tikhonenko, F. V.; Ziborov, V. S.; Dolgorobodov, A. Yu.; Petrov, O. F.; Gadzhieva, O. A.; Bashiryan, B. A.; Shimansky, V. N.; Potoldykov, N. V.; Enikeev, D. V.; Usachev, D. Yu.; Archakov, A. I. Nanoribbon-Based Electronic Detection of a Glioma-Associated Circular MiRNA. *Biosensors* **2021**, *11* (7), 237. <https://doi.org/10.3390/bios11070237>.

32. Ivanov, Y. D.; Malsagova, K. A.; Pleshakova, T. O.; Galiullin, R. A.; Kozlov, A. F.; Shumov, I. D.; Popov, V. P.; Kapustina, S. I.; Ivanova, I. A.; Isaeva, A. I.; Tikhonenko, F. V.; Kushlinskii, N. E.; Alferov, A. A.; Tatur, V. Yu.; Ziborov, V. S.; Petrov, O. F.; Glukhov, A. V.; Archakov, A. I. Aptamer-Sensitized Nanoribbon Biosensor for Ovarian Cancer Marker Detection in Plasma. *Chemosensors* **2021**, *9* (8), 222. <https://doi.org/10.3390/chemosensors9080222>.

33. Malsagova, K. A.; Pleshakova, T. O.; Galiullin, R. A.; Kozlov, A. F.; Shumov, I. D.; Popov, V. P.; Tikhonenko, F. V.; Glukhov, A. V.; Ziborov, V. S.; Petrov, O. F.; Fortov, V. E.; Archakov, A. I.; Ivanov, Y. D. Highly Sensitive Detection of CA 125 Protein with the Use of an N-Type Nanowire Biosensor. *Biosensors* **2020**, *10* (12), 210. <https://doi.org/10.3390/bios10120210>.

34. Malsagova, K. A.; Ivanov, Y. D.; Pleshakova, T. O.; Kaysheva, A. L.; Shumov, I. D.; Kozlov, A. F.; Archakov, A. I.; Popov, V. P.; Fomin, B. I.; Latyshev, A. V. A SOI-Nanowire Biosensor for the Multiple Detection of D-NFATc1 Protein in the Serum. *Anal. Methods* **2015**, *7* (19), 8078–8085. <https://doi.org/10.1039/C5AY01866H>.

35. Shi, S.; Yu, X.; Gao, Y.; Xue, B.; Wu, X.; Wang, X.; Yang, D.; Zhu, H. Inhibition of Hepatitis C Virus Production by Aptamers against the Core Protein. *J. Virol.* **2014**, *88* (4), 1990–1999. <https://doi.org/10.1128/JVI.03312-13>.

36. Popov, V. P.; Antonova, A. I.; Frantsuzov, A. A.; Safronov, L. N.; Feofanov, G. N.; Naumova, O. V.; Kilanov, D. V. Properties of Silicon-on-Insulator Structures and Devices. *Semiconductors* **2001**, *35* (9), 1030–1037. <https://doi.org/10.1134/1.1403567>.

37. Ivanov, Y. D.; Goldaeva, K. V.; Malsagova, K. A.; Pleshakova, T. O.; Galiullin, R. A.; Popov, V. P.; Kushlinskii, N. E.; Alferov, A. A.; Enikeev, D. V.; Potoldykov, N. V.; Archakov, A. I. Nanoribbon Biosensor in the Detection of MiRNAs Associated with Colorectal Cancer. *Micromachines* **2021**, *12* (12), 1581. <https://doi.org/10.3390/mi12121581>.

38. Yamada, K.; Yoshii, S.; Kumagai, S.; Fujiwara, I.; Nishio, K.; Okuda, M.; Matsukawa, N.; Yamashita, I. High-Density and Highly Surface Selective Adsorption of Protein–Nanoparticle Complexes by Controlling Electrostatic Interaction. *Jpn. J. Appl. Phys.* **2006**, *45*, 4259–4264. <https://doi.org/10.1143/JJAP.45.4259>.

39. Malsagova, K. A.; Pleshakova, T. O.; Popov, V. P.; Kupriyanov, I. N.; Galiullin, R. A.; Kozlov, A. F.; Shumov, I. D.; Kaysheva, A. L.; Tikhonenko, F. V.; Archakov, A. I.; Ivanov, Y. D. Optical Monitoring of the Production Quality of Si-Nanoribbon Chips Intended for the Detection of ASD-Associated Oligonucleotides. *Micromachines (Basel)* **2021**, *12* (2), 147. <https://doi.org/10.3390/mi12020147>.

40. Ivanov, Y. D.; Malsagova, K. A.; Popov, V. P.; Kupriyanov, I. N.; Pleshakova, T. O.; Galiullin, R. A.; Ziborov, V. S.; Dolgorobodov, A. Y.; Petrov, O. F.; Miakonkikh, A. V.; Rudenko, K. V.; Glukhov, A. V.; Smirnov, A. Y.; Usachev, D. Y.; Gadzhieva, O. A.; Bashiryan, B. A.; Shimansky, V. N.; Enikeev, D. V.; Potoldykova, N. V.; Archakov, A. I. Micro-Raman Characterization of Structural Features of High-k Stack Layer of SOI Nanowire Chip, Designed to Detect Circular RNA Associated with the Development of Glioma. *Molecules* **2021**, *26* (12), 3715. <https://doi.org/10.3390/molecules26123715>.

41. Ahoulou, S.; Perret, E.; Nedelec, J.-M. Functionalization and Characterization of Silicon Nanowires for Sensing Applications: A Review. *Nanomaterials (Basel)* **2021**, *11* (4), 999. <https://doi.org/10.3390/nano11040999>.

42. Ivanov, Yu. D.; Pleshakova, T. O.; Malsagova, K. A.; Kozlov, A. F.; Kaysheva, A. L.; Shumov, I. D.; Galiullin, R. A.; Kurbatov, L. K.; Popov, V. P.; Naumova, O. V.; Fomin, B. I.; Nasimov, D. A.; Aseev, A. L.; Alferov, A. A.; Kushlinsky, N. E.; Listitsa, A. V.; Archakov, A. I. Detection of Marker MiRNAs in Plasma Using SOI-NW Biosensor. *Sensors and Actuators B: Chemical* **2018**, *261*, 566–571. <https://doi.org/10.1016/j.snb.2018.01.153>.

43. Laborde, C.; Pittino, F.; Verhoeven, H. A.; Lemay, S. G.; Selmi, L.; Jongsma, M. A.; Widdershoven, F. P. Real-Time Imaging of Microparticles and Living Cells with CMOS Nanocapacitor Arrays. *Nat Nanotechnol* **2015**, *10* (9), 791–795. <https://doi.org/10.1038/nnano.2015.163>.

44. Stern, E.; Wagner, R.; Sigworth, F. J.; Breaker, R.; Fahmy, T. M.; Reed, M. A. Importance of the Debye Screening Length on Nanowire Field Effect Transistor Sensors. *Nano Lett.* **2007**, *7* (11), 3405–3409. <https://doi.org/10.1021/nl071792z>.

45. Hahm, J.; Lieber, C. M. Direct Ultrasensitive Electrical Detection of DNA and DNA Sequence Variations Using Nanowire Nanosensors. *Nano Lett.* **2004**, *4* (1), 51–54. <https://doi.org/10.1021/nl034853b>.

46. Elfström, N.; Juhasz, R.; Sychugov, I.; Engfeldt, T.; Karlström, A.E.; Linnros, J. Surface Charge Sensitivity of Silicon Nanowires: Size Dependence. *Nano Lett.* **2007**, *7*, 2608–2612. <https://doi.org/10.1021/nl0709017>.

47. Kamili, S.; Drobniuc, J.; Araujo, A. C.; Hayden, T. M. Laboratory Diagnostics for Hepatitis C Virus Infection. *Clin Infect Dis* **2012**, *55 Suppl 1*, S43–48. <https://doi.org/10.1093/cid/cis368>.

48. Khudur Al-Nassary, M. S.; Mahdi, B. M. Study of Hepatitis C Virus Detection Assays. *Annals of Medicine and Surgery* **2018**, *36*, 47–50. <https://doi.org/10.1016/j.amsu.2018.10.002>.

49. Feld, J. J. Hepatitis C Virus Diagnostics: The Road to Simplification. *Clinical Liver Disease* **2018**, *12* (5), 125–129. <https://doi.org/10.1002/cld.760>.

50. Warkad, S. D.; Nimse, S. B.; Song, K.-S.; Kim, T. HCV Detection, Discrimination, and Genotyping Technologies. *Sensors (Basel)* **2018**, *18* (10), 3423. <https://doi.org/10.3390/s18103423>.

51. Hosseini-Moghaddam, S.; Iran-Pour, E.; Rotstein, C.; Husain, S.; Lilly, L.; Renner, E.; Mazzulli, T. Hepatitis C Core Ag and Its Clinical Applicability: Potential Advantages and Disadvantages for Diagnosis and Follow-up?: Clinical Applicability of HCVcAg. *Rev. Med. Virol.* **2012**, *22* (3), 156–165. <https://doi.org/10.1002/rmv.717>.

52. Ghany, M. G.; Strader, D. B.; Thomas, D. L.; Seeff, L. B.; American Association for the Study of Liver Diseases. Diagnosis, Management, and Treatment of Hepatitis C: An Update. *Hepatology* **2009**, *49* (4), 1335–1374. <https://doi.org/10.1002/hep.22759>.

53. Saludes, V.; González, V.; Planas, R.; Matas, L.; Ausina, V.; Martró, E. Tools for the Diagnosis of Hepatitis C Virus Infection and Hepatic Fibrosis Staging. *World J Gastroenterol* **2014**, *20* (13), 3431–3442. <https://doi.org/10.3748/wjg.v20.i13.3431>.

54. Coulibaly, M.; Maiga, B.; Samaké, D.; Diawara, M.; Traoré, M.; Sagara, V.; Traoré, B.; Guindo, O.; Dolo, A. Assessment of Rapid Diagnostic Tests Algorithms in Transfusion Medicine Setting. *ABC* **2021**, *11* (01), 52–63. <https://doi.org/10.4236/abc.2021.111005>.

55. Amborkar, P.; Wang, Z.; Ko, H.; Lee, S.; Koo, K.; Kim, K.; Cho, D. Nanowire-Based Biosensors: From Growth to Applications. *Micromachines* **2018**, *9* (12), 679. <https://doi.org/10.3390/mi9120679>.

56. Mohd Azmi, M. A.; Tehrani, Z.; Lewis, R. P.; Walker, K.-A. D.; Jones, D. R.; Daniels, D. R.; Doak, S. H.; Guy, O. J. Highly Sensitive Covalently Functionalised Integrated Silicon Nanowire Biosensor Devices for Detection of Cancer Risk Biomarker. *Biosensors and Bioelectronics* **2014**, *52*, 216–224. <https://doi.org/10.1016/j.bios.2013.08.030>.

57. Thiviyananthan, V.; Gorenstein, D. G. Aptamers and the next Generation of Diagnostic Reagents. *Proteomics Clin Appl* **2012**, *6* (11–12), 563–573. <https://doi.org/10.1002/prca.201200042>.

disclaim responsibility for any injury to people or property resulting from any ideas, methods, instructions or products referred to in the content.